

Article

Fabrication and Characterization of Antimicrobial Magnetron Cospattered TiO₂/Ag/Cu Composite Coatings

Dilyana Gospodanova ¹, Iliana Ivanova ² and Todorka Vladkova ^{3,*}

¹ Faculty of Electrical Engineering, Technical University, 8 "Kliment Ohridski" Blvd, 1756 Sofia, Bulgaria; dilianang@tu-sofia.bg

² Biological Faculty, Sofia University, "St. Kl. Ohridski", 8 "Dragan Tsankov" Blvd, 1164 Sofia, Bulgaria; ilivanova@abv.bg

³ Laboratory for Advanced Materials Research, University of Chemical Technology and Metallurgy, 8 "Kliment Ohridski" Blvd, 1756 Sofia, Bulgaria

* Correspondence: tvg@uctm.edu; Tel.: +359-2-887839374

Abstract: The aim of this study was to prepare TiO₂/Ag/Cu magnetron co-sputtered coatings with controlled characteristics and to correlate them with the antimicrobial activity of the coated glass samples. The elemental composition and distribution, surface morphology, wettability, surface energy and its component were estimated as the surface characteristics influencing the bioadhesion. Well expressed, specific, Ag/Cu concentration-dependent antimicrobial activity in vitro was demonstrated toward Gram-negative and Gram-positive standard test bacterial strains both by diffusion 21 assay and by Most Probable Number of surviving cells. Direct contact and eluted silver/copper nanoparticles killing were experimentally demonstrated as a mode of the antimicrobial action of the studied TiO₂/Ag/Cu thin composite coatings. It is expected that they would ensure a broad spectrum bactericidal activity during the indwelling of the coated medical devices and for at least 12 h after that, with the supposition that the benefits will be over a longer time.



Citation: Gospodanova, D.; Ivanova, I.; Vladkova, T. Fabrication and Characterization of Antimicrobial Magnetron Cospattered TiO₂/Ag/Cu Composite Coatings. *Coatings* **2021**, *11*, 473. <https://doi.org/10.3390/coatings11040473>

Academic Editor: Ajay Vikram Singh

Received: 26 March 2021

Accepted: 15 April 2021

Published: 17 April 2021

Publisher's Note: MDPI stays neutral with regard to jurisdictional claims in published maps and institutional affiliations.



Copyright: © 2021 by the authors. Licensee MDPI, Basel, Switzerland. This article is an open access article distributed under the terms and conditions of the Creative Commons Attribution (CC BY) license (<https://creativecommons.org/licenses/by/4.0/>).

1. Introduction

The increasing number of medical devices-associated infections and the microbial resistance to conventional drugs treatments raised the need for the efficient antimicrobial protection of medical devices, which is especially important for those in the urinary tract [1]. Surface coating technologies are a tool to mitigate the problem. They usually aim at the creation of an antiadhesive surface that does not allow the attachment of microbial cells and hence inhibits the initial stage of the biofilm formation; or at the creation of a contact killing or antibacterial agent delivering surface. Antibiotics, antimicrobial peptides and other organic compounds, such as enzymes, polymer gels, carbon materials, metal, metal oxide nanoparticles and ions and others, are in use in the development of antimicrobial coatings [2,3].

Due to their advantages, like low-toxicity, biocompatibility, high stability, etc. functional nanostructured TiO₂ coatings are one of the most investigated among the metal oxide coatings [4–7]. Doping with other metal or/and metal oxide nanoparticles (NPs) to enhance their antimicrobial activity is widely investigated. Ag and Cu (which have been known for centuries for their good antibacterial properties) are one of the most often used. According to some current reports, Cu is also active against viruses [8–11]. The quantitative control over the incorporated Ag and Cu amount allows the realizing of both antibacterial activity and biocompatibility [12,13].

The development of Ag-doped TiO₂ coatings and composites with improved antimicrobial activity continues [14–24]. Direct contact and released silver NPs and ions killing

are proposed as a basis of the bactericidal action of such coatings [23]. The development of Cu-doped TiO₂ coatings and composites also continues, and a large variety of such coatings with improved antimicrobial activity are reported in the literature [25–40].

Our short review demonstrated that different techniques are in use for preparation and deposition of antimicrobial coatings, each one with its own advantages and disadvantages. Among them are the Chemical Vapor Deposition (CVD) in different modes [18–24]; the sol-gel method [41–43]; the sputtering of multilayered and nanocomposite thin films [3,44–49]; and others. Magnetron sputtering is preferred for the fabrication of antimicrobial coatings because of its advantages. This is a dry method that ensures precise control over the plasma processing parameters and allows good control over the thickness of the deposited layers, their chemistry, charge, structure, morphology, hydrophilic/hydrophobic balance, etc. The long-term antimicrobial activity of the magnetron sputtered thin films, which could be deposited on any surface, is another advantage [48].

Triple TiO₂/Ag/Cu magnetron cosputtered thin composite coatings are scarcely studied although they hold promise for a broad spectrum antibacterial activities due to the combination of three types biologically active nanoparticles: TiO₂, Ag and Cu. In a former paper [50] we reported some preliminary results about the bioactivity of such coatings without correlation to their characteristics. Therefore, the fabrication of and search for a correlation between the biological activity and the characteristics of magnetron cosputtered TiO₂/Ag/Cu composite coatings became the subject of this investigation, with our final aim being to demonstrate the ability of such coatings to be adjusted to the antimicrobial protection requirements of different medical devices.

2. Materials and Methods

2.1. Preparation of Coated Samples

Alcatel DION 450 magnetron installation, equipped with rotary and diffusion vacuum pumps and cylindrical glass camera was used to deposit thin coatings (50–60 nm, Tailor Hobzon profilometer, Leicester, UK) on glass substrates (20 mm × 20 mm × 1 mm). RF magnetron cosputtering was performed under the following operation conditions: power of 50 W; vacuum in the sputtering chamber of 10⁻³ Pa before the film deposition; 0.8 Pa argon gas atmosphere; distance between the target and substrate of 7.5 cm; Ag- and Cu-plates, placed together with TiO₂ target in its erosion zone; without heating. The glass substrates were 76 preliminary treated with Piranha etch, H₂SO₄:H₂O₂ (30%) = 3:1, to improve their adhesion with the coatings. The area of TiO₂ was of 750 mm², whereas that of both Ag and Cu sheds was varied between 40 and 190 mm² to obtain thin coatings with different Ag and Cu content was confirmed by Energy Dispersive X-ray Detector (EDX) analysis. Five magnetron cosputtered TiO₂/Ag/Cu coatings, deposited on glass substrates were selected for this investigation to evaluate the influence of the Ag and Cu content on their characteristics and antibacterial activity: three of them with varied Cu content at almost equal Ag amount (Samples 1, 2 and 3) as well as three of them with varied Ag content at almost equal Cu amount (Samples 3, 4 and 5). The exact content of Ti, Ag and Cu, at.%, was evaluated from the detailed Ti2p, Ag3d and Cu2p X-ray Photoelectron Spectroscopy (XPS) spectra of the corresponding coating.

2.2. Characterization the Coated Test Samples

2.2.1. X-ray Photoelectron Spectroscopy (XPS)

Kratos AXIS Supra spectrometer (Manchester, UK) with a monochromatic Al X-ray source under vacuum better than 10⁻⁸ Pa at 90° take-off angle was used for elemental analysis of the coatings. It started with a survey scan from 0 to 1200 eV, pass energy of 160 eV at steps of 0.5 eV with 1 sweep. For high resolution analyses the sweep number was increased, the pass energy was lowered to 20 eV at steps of 100 meV. The C1s photoelectron line at 285 eV was used for calibration of the spectra. Ag content, atomic %, was calculated from the area of the detailed Ag 3d3/2 and Ag 3d5/2 peaks; that of Cu—from the area of Cu2p3/2 and Cu2p1/2 peaks.

2.2.2. Scanning Electron Microscope (SEM) and SEM/EDX

SEM (JEOL, model JSM-35 CF, Tokyo, Japan) apparatus was used to observe the morphological features of the studied magnetron cosputtered TiO₂/Ag/Cu composite coatings as well as of *E. coli* cells damaging and contact killing by them. The samples were gold sputtered coated and viewed in the second electron mode with field emission gun.

Lira/TEScan SEM (Brucker, Berlin, Germany) apparatus equipped with Quantax 200 EDX detector was used for preliminary evaluation of the elemental composition and to observe elements' distribution in the studied magnetron cosputtered TiO₂/Ag/Cu thin composite coating.

2.3. In Vitro Antibacterial Activity

2.3.1. Microbial Strains

Microbial strains used in this investigation were 3 standard Gram-negative bacteria: *Escherichia coli* 3548 NBIMCC (ATCC 10536); *Pseudomonas putida* 1090 NBIMCC (ATCC 12633); *Pseudomonas aeruginosa* ATCC 27853 NBIMCC (DSM4224) and 2 Gram-positive bacteria: *Bacillus cereus* ATTC 11778 and *Staphylococcus epidermidis* 3486, NBIMCC (ATCC 12228), all supplied by the National Bank of Industrial Microorganisms and Cells Cultures (NBIMCC). Every test culture was grown in a nutrient broth (Conda, Torrejon de Ardoz, Spain) on a rotary shaker (180 rpm) at 37 °C overnight followed by a subculturing of the bacteria in fresh medium until optical density reached 0.02–0.05, detected spectrophotometrically at 610 nm (0.5 McFarland). The bacterial suspension (100 µL) was used for inoculation of nutrient agar in Petri dishes.

2.3.2. Agar Diffusion Assay

Agar diffusion assay was used for a fast antibacterial activity screening of the studied TiO₂/Ag/Cu coatings. The aliquots of 100 µL microbial suspension were randomly spread on a solid nutrient medium (Conda, Spain). The coated samples were sterilized by UV-irradiation for 30 min and placed on inoculated agar. The inoculated dishes were kept in refrigerator at 4 °C for 2 h to allow the diffusion of nanoparticles from the corresponding thin coating in the agar and after that cultivated for 24–48 h at 37 °C. The formed sterile zones around the samples were measured in mm.

2.3.3. Cell Growth Inhibition (Most Probable Number of Surviving Cells Test)

The Most Probable Number (MPN) of surviving cells [49] was used to evaluate the inhibition of bacterial growth above the coated samples, placed in Corning® Costar® (Northeim, Germany) TC-Treated, 6 well polystyrene plates. The cultivation of bacteria was performed in organic nutrient medium (NB, Conda, Spain) that is most suitable for bacterial growth and multiplication, to reliably prove the antibacterial effect. The concentration of the bacterial cells was 10⁵–10⁷ CFU·mL⁻¹.

OD of bacterial suspension, in absence (control) and in presence of coated sample, was measured every hour ($\lambda = 610$ nm, Spekol-11, Carl Zeiss, Jena, Germany). For the MPN test, 10-fold dilutions were made in intervals of 2 h. Surviving cells were determined at different time points as described earlier [50]. All results are average of 3 measurements.

2.3.4. SEM Observation of *E. coli* on Coated Samples

E. coli on TiO₂/Ag/Cu coated glass samples were observed after incubation in nutrient medium for 6 h, followed by distilled water rinsing and drying for 12 h under room conditions. Cathode sputtering of gold coating under vacuum in argon atmosphere was made before the SEM observation (Joel JSM 5510, Tokio, Japan).

3. Results

To evaluate the impact of both Ag and Cu content on the antibacterial activity of the TiO₂/Ag/Cu composite coatings, five coated samples were selected for this investigation with varied Cu content at almost equal Ag content (Samples 1, 2, and 3) or with varied

Ag content at almost equal Cu content (Samples 3, 4, and 5), based on EDX analyses. The exact content of Ti, Ag and Cu, in at.%, estimated from the corresponding detailed Ti2p, Ag3d and Cu2p XPS spectra, are presented in Table 1. Surface characterization of the studied coatings was carried out beforehand to evaluate their antimicrobial activity since the microbial adhesion depends on surface characteristics like surface chemistry and topography, hydrophilic/hydrophobic balance, surface energy, etc. [51–57].

Table 1. Elemental composition of cosputtered $\text{TiO}_2/\text{Ag}/\text{Cu}$ nanocomposite coatings (from XPS) prepared under varied surface area of the Ag and Cu sheds.

| Sample No. | C1s, at.% | Ti2p, at.% | Ag3d, at.% | Cu2p, at.% |
|------------|-----------|------------|------------|------------|
| 1. | 4.12 | 30.78 | 14.7 | 13.0 |
| 2. | 3.18 | 31.00 | 14.2 | 17.9 |
| 3. | 5.25 | 27.31 | 14.3 | 21.3 |
| 4. | 8.21 | 26.48 | 18.6 | 22.4 |
| 5. | 6.33 | 24.04 | 23.1 | 21.6 |

3.1. Elemental Composition (XPS Analysis)

In the survey XPS spectra of all studied $\text{TiO}_2/\text{Ag}/\text{Cu}$ coated samples, the characteristic peaks of the elements C, O, Ti, Si and Ag were presented; the elements O, Ti, Ag and Cu originating from the cosputtered $\text{TiO}_2/\text{Ag}/\text{Cu}$ coatings and carbon, originating from the air. The results of the quantitative elemental analysis for Ti, Ag and Cu presenting in the magnetron cosputtered $\text{TiO}_2/\text{Ag}/\text{Cu}$ thin composite coatings, based on detailed Ti2p, Ag3d and Cu2p XPS spectra, are presented in Table 1.

It is evident that samples 1, 2 and 3 contain almost equal Ag amounts of about 14 at.%, whereas the Cu content varies between 13 at.% and 21 at.%; samples 3, 4, and 5 contain almost equal Cu amounts of 21 at.%–22 at.%, whereas the Ag content varies between 14 at.% and 23 at.%. These five samples were used in the further investigations.

3.2. Elements Distribution (EDX)

The elements' distribution is seen in Figure 1, which presents the EDX spectrum (a), an integrated map (b) and the individual elements' distribution (Ti, Ag, and Cu (c, d, e, respectively)) of coated glass Sample 5— $\text{TiO}_2/\text{Ag}_{23.1}\text{ at.}/\text{Cu}_{21.6}\text{ at.}\%$.

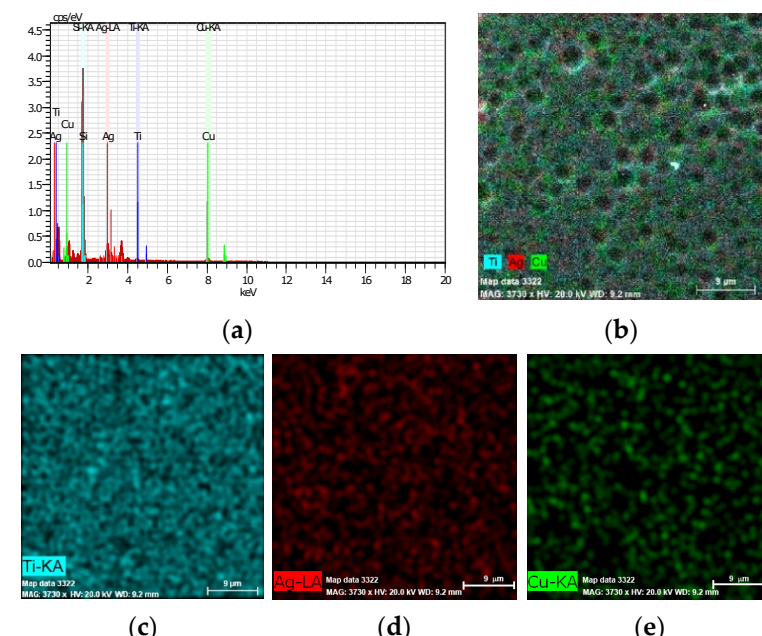


Figure 1. EDX spectrum (a), integrated map of Ti, Ag and Cu distribution (b) and maps of the individual elements Ti (c), Ag (d), Cu (e) distribution in Sample 5— $\text{TiO}_2/\text{Ag}_{23.1}\text{ at.}/\text{Cu}_{21.6}\text{ at.}\%$.

It is evident that all three elements (Ti, Ag and Cu) form chainlike aggregates (Figure 1c–e), specifically integrated in the $\text{TiO}_2/\text{Ag}_{23.1}\text{ at.\%}/\text{Cu}_{21.6}\text{ at.\%}$ coating to form dark depression wells, visible in the integrated map, Figure 1b. This picture is characteristic for all studied $\text{TiO}_2/\text{Ag}/\text{Cu}$ coatings, including Samples 1–4, and therefore their maps are not presented here.

3.3. Surface Morphology (SEM)

The typical surface morphology of $\text{TiO}_2/\text{Ag}_{23.1}\text{ at.\%}/\text{Cu}_{21.6}\text{ at.\%}$ coated Sample 5 (Figure 2b) and that of TiO_2 coated one (Figure 2a), for comparison, is presented in Figure 2. The TiO_2 coated surface is flat (Figure 2a) whereas that of $\text{TiO}_2/\text{Ag}_{23.1}\text{ at.\%}/\text{Cu}_{21.6}\text{ at.\%}$ coated Sample 5 (b) characterizes by arrangements of chaotically distributed chainlike aggregates of Ag/Cu particles with different shapes and sizes, most of them submicron, which form dark walls, easily visible in Figure 1b. Such Ag and Cu particles' distribution is characteristic for all $\text{TiO}_2/\text{Ag}/\text{Cu}$ magnetron cosputtered coatings. Therefore, their pictures are not presented here.

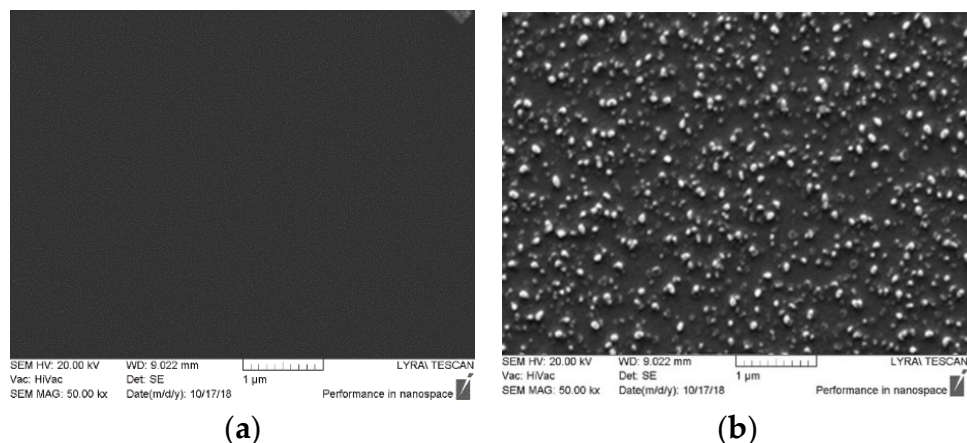


Figure 2. Morphology of: (a) TiO_2 magnetron sputtered coating on glass substrate ($\times 5000$); (b) $\text{TiO}_2/\text{Ag}_{23.1}\text{ at.\%}/\text{Cu}_{21.6}\text{ at.\%}$ magnetron cosputtered coating on glass substrate, Sample 5.

3.4. Water Contact Angle, WCA, Surface Energy, E and its Polar, E_p and Disperse, E_d Parts

As is evident from Table 2, the studied samples demonstrate slight deviations in the WCA (of $63.0\text{--}69.1^\circ$) and the surface energy, E (of 34.96 mN/m – 39.21 mN/m), remaining in the region of moderate hydrophilic surfaces. This indicates that the insignificant impact of the surface hydrophilic/hydrophobic balance and surface energy could be expected on the initial microbial adhesion [58].

Table 2. Water contact angle, WCA, surface energy, E and its polar E_p , and disperse part, E_d of $\text{TiO}_2/\text{Ag}/\text{Cu}$ composite coatings both with almost equal Ag content and varied Cu content (Samples 1, 2 and 3) or with almost equal copper content and varied silver content (samples 2, 4, and 5).

| Samples | WCA, $^\circ$ | $E, \text{mN/m}$ | $E_p, \text{mN/m}$ | $E_d, \text{mN/m}$ |
|--|-----------------|------------------|--------------------|--------------------|
| Sample 1- $\text{TiO}_2/\text{Ag}_{14.7}\text{ at.\%}/\text{Cu}_{13.0}\text{ at.\%}$ | 62.2 ± 0.63 | 36.12 | 11.10 | 25.02 |
| Sample 2- $\text{TiO}_2/\text{Ag}_{14.0}\text{ at.\%}/\text{Cu}_{17.9}\text{ at.\%}$ | 61.9 ± 0.36 | 38.03 | 12.33 | 25.70 |
| Sample 3- $\text{TiO}_2/\text{Ag}_{14.3}\text{ at.\%}/\text{Cu}_{21.3}\text{ at.\%}$ | 63.0 ± 0.71 | 35.92 | 10.12 | 25.80 |
| Sample 4- $\text{TiO}_2/\text{Ag}_{18.6}\text{ at.\%}/\text{Cu}_{22.4}\text{ at.\%}$ | 60.3 ± 0.52 | 39.21 | 11.20 | 28.01 |
| Sample 5- $\text{TiO}_2/\text{Ag}_{23.1}\text{ at.\%}/\text{Cu}_{21.6}\text{ at.\%}$ | 69.1 ± 0.89 | 34.96 | 17.90 | 26.06 |

3.5. In Vitro Antimicrobial Activity

3.5.1. Diffusion Test

The diffusion test was employed for quick antibacterial screening of the studied $\text{TiO}_2/\text{Ag}/\text{Cu}$ magnetron cosputtered coatings. The results are presented in Table 3.

Table 3. Antimicrobial activity toward Gram-negative and Gram-positive microbial strains (as a sterile zone, mm; by agar diffusion test) of $\text{TiO}_2/\text{Ag}/\text{Cu}$ magnetron cosputtered thin coatings depending on the Cu-content at almost equal Ag content (Samples 1, 2, and 3) and depending on Ag content at almost equal Cu content (Samples 3, 4, and 5).

| Sample No. | Sterile Zone, mm | | | |
|--|------------------|----------------------|-----------------------|----------------------|
| | <i>E. coli</i> | <i>P. aeruginosa</i> | <i>S. epidermidis</i> | <i>S. holeresius</i> |
| Sample 1- $\text{TiO}_2/\text{Ag}_{14.7}\text{ at.\%}/\text{Cu}_{13.0}\text{ at.\%}$ | 1 ± 0.5 | 3 ± 0.5 | 2 ± 0.5 | 2 ± 0.5 |
| Sample 2- $\text{TiO}_2/\text{Ag}_{14.0}\text{ at.\%}/\text{Cu}_{17.9}\text{ at.\%}$ | 3 ± 0.5 | 4 ± 0.5 | 5 ± 0.5 | 4 ± 0.5 |
| Sample 3- $\text{TiO}_2/\text{Ag}_{14.3}\text{ at.\%}/\text{Cu}_{21.3}\text{ at.\%}$ | 2 ± 0.5 | 4 ± 0.5 | 5 ± 0.5 | 4 ± 0.5 |
| Sample 4- $\text{TiO}_2/\text{Ag}_{18.6}\text{ at.\%}/\text{Cu}_{22.4}\text{ at.\%}$ | 5 ± 0.5 | 6 ± 0.5 | 7 ± 0.5 | 8 ± 0.5 |
| Sample 5- $\text{TiO}_2/\text{Ag}_{23.1}\text{ at.\%}/\text{Cu}_{21.6}\text{ at.\%}$ | 6 ± 0.5 | 8 ± 0.5 | 9 ± 0.5 | 9 ± 0.5 |

The data in Table 3 demonstrate a specific concentration of both the Ag- and Cu-dependent antimicrobial activity of the studied $\text{TiO}_2/\text{Ag}/\text{Cu}$ composite magnetron cosputtered coatings toward different microbial strains. The bactericidal activity of the test microbial species: (*E. coli*, *P. aeruginosa*, *S. epidermidis* and *S. holeresius*) is different on coatings with the same composition (Table 3, the sterile zones' data in the rows). The sterile zones are different also for the test bacteria on the $\text{TiO}_2/\text{Ag}/\text{Cu}$ composite coatings containing different amounts of both Ag and Cu (Table 3, the sterile zones' data in the columns). The inhibition zones of the studied bacteria are increasingly enlarged with the increasing Ag content (compare Samples 3, 4 and 5) and less enlarged with the increasing Cu content (compare Samples 1, 2 and 3), which indicates a stronger bactericidal effect of the Ag NPs as compared to that of the Cu NPs. The largest sterile zones appeared for all microbial strains in Sample 5— $\text{TiO}_2/\text{Ag}_{23.1}\text{ at.\%}/\text{Cu}_{21.6}\text{ at.\%}$ —the coating with the highest content of both Ag and Cu (Table 3, the last row).

3.5.2. Cell Growth Inhibition

Two microbial strains, Gram-negative, *E. coli* and Gram-positive, *S. epidermidis* were used to study the cell growth inhibition on the studied $\text{TiO}_2/\text{Ag}/\text{Cu}$ cosputtered composition coatings with different Cu content and almost equal Ag content as well as with different Ag content at almost equal Cu content by MPN of the surviving cells. The dynamic of the *E. coli* growth inhibition is presented in Figure 3.

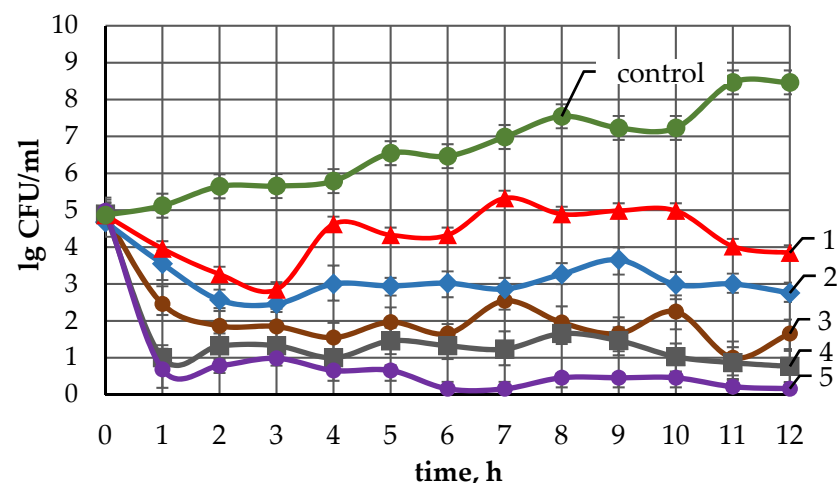


Figure 3. *E. coli* growth inhibition in presence of: (1) Sample 1- $\text{TiO}_2/\text{Ag}_{14.7}\text{ at.\%}/\text{Cu}_{13.0}\text{ at.\%}$; (2) Sample 2- $\text{TiO}_2/\text{Ag}_{4.0}\text{ at.\%}/\text{Cu}_{17.9}\text{ at.\%}$; (3) Sample 3- $\text{TiO}_2/\text{Ag}_{14.3}\text{ at.\%}/\text{Cu}_{21.3}\text{ at.\%}$; (4) Sample 4- $\text{TiO}_2/\text{Ag}_{18.6}\text{ at.\%}/\text{Cu}_{22.4}\text{ at.\%}$; (5) Sample 5- $\text{TiO}_2/\text{Ag}_{23.1}\text{ at.\%}/\text{Cu}_{21.6}\text{ at.\%}$; or in absence of sample—control.

Figure 3 demonstrates a well expressed antimicrobial activity of $\text{TiO}_2/\text{Ag}/\text{Cu}$ coatings against *E. coli*, dependent on the concentration of both Ag and Cu. The significant inhibition of the *E. coli* growth happens in the first 1–2 h of exposure to the coated samples: the sharp slope of the curves 1–5 in the range of 1–3 h. The positions of curve 1, curve 2, and curve 3 in Figure 3 demonstrate the Cu concentration-dependent antibacterial activity of the coatings, containing almost equal amounts of Ag (about 14 at.-%), and varied Cu content at: 13.0 at.-% (curve 1), 17.9 at.-% (curve 2), and 21.3 at.-% (curve 3)—the increase in the Cu content leads to a stronger suppression of *E. coli* growth and the MPN of the living cells decreases. Similar dependence of the antimicrobial activity is observed for the $\text{TiO}_2/\text{Ag}/\text{Cu}$ coatings containing almost equal Cu amounts of about 21 at.-%–22 at.% and varied Ag content at: 14.3 at.-% (curve 3), 18.6 at.-% (curve 4), and 23.1 at.-% (curve 5). The MPN of the active cells presented by curve 4 is lower than that of the previous concentration of nanoparticles shown by curve 3 and curve 5 is below curve 4. The inhibitory effect toward *E. coli* is most strongly expressed in Sample 5 (curve 5), in which the amounts of both Ag and Cu in the $\text{TiO}_2/\text{Ag}/\text{Cu}$ coating are maximal: 23.1 at.-% and 21.6 at.-%, respectively. The MPN of the surviving *E. coli* cells tends to zero in this case. The data presented in Figure 3 (MPN of surviving cells) are in accordance with those obtained by the diffusion assay, presented in Table 3. The MPN of the surviving cells and the diffusion assay demonstrate good congruence and increased inhibitory effect against *E. coli* with the increase in the concentration.

Figure 4 represents the inhibitory effect of the same $\text{TiO}_2/\text{Ag}/\text{Cu}$ composite coatings toward *S. epidermidis*.

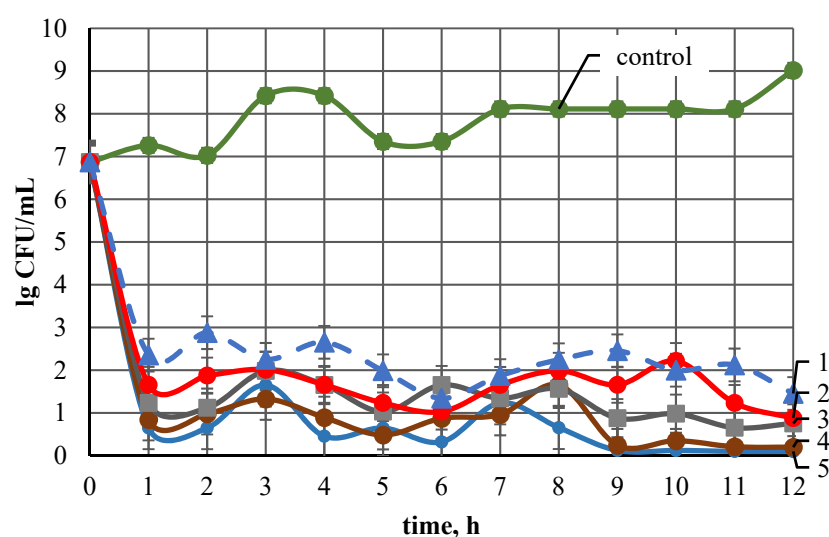


Figure 4. *S. epidermidis* growth inhibition in presence of: (1) Sample 1- $\text{TiO}_2/\text{Ag}_{14.7}\text{ at.}\%/\text{Cu}_{13.0}\text{ at.}\%$; (2) Sample 2- $\text{TiO}_2/\text{Ag}_{4.0}\text{ at.}\%/\text{Cu}_{17.9}\text{ at.}\%$; (3) Sample 3- $\text{TiO}_2/\text{Ag}_{14.3}\text{ at.}\%/\text{Cu}_{21.3}\text{ at.}\%$; (4) Sample 4- $\text{TiO}_2/\text{Ag}_{18.6}\text{ at.}\%/\text{Cu}_{22.4}\text{ at.}\%$; (5) Sample 5- $\text{TiO}_2/\text{Ag}_{23.1}\text{ at.}\%/\text{Cu}_{21.6}\text{ at.}\%$; or in absence of sample—control.

Figure 4 demonstrates a very well expressed antimicrobial activity of $\text{TiO}_2/\text{Ag}/\text{Cu}$ coatings against *S. epidermidis*, depending on the concentration of both Ag and Cu. A comparison of the group of curves 1–5 in Figure 3, to group of curves 1–5 in Figure 4 demonstrates the faster death and an MPN more closely approaching zero of the surviving cells in the second one (Figure 4), which indicates the higher sensitivity of *S. epidermidis* compared to *E. coli*, to both Ag NPs and Cu NPs. The strong inhibition of the *S. epidermidis* growth happens in the first 1–2 h of exposure to the coated samples, as indicated by the sharp slope of the curves 1–5 in Figure 4 in this time interval. The position of curves 1, 2 and 3 in Figure 4 (near each to other) demonstrates the slight increase in the antimicrobial activity with the increase in the Cu NPs concentration of the coatings, containing the same amount Ag of about 14 at.-%, and varied Cu content: from 13.0 at.-% (curve 1) to 17.9 at.-% (curve 2) and 21.6 at.-% (curve 3). The increase in the Ag NPs content from 14.3

at.% (curve 3); to 18.6 at.% (curve 4) and 23.1 at.% (curve 5) in the studied $\text{TiO}_2/\text{Ag}/\text{Cu}$ composite coatings at almost equal to Cu NPs content at 22 at.%–23 at.%, increases their activity against *S. epidermidis*, as indicated by the positions of the curves 3, 4 and 5 in Figure 4. The inhibitory effect toward *S. epidermidis* cell is most strongly expressed at Sample 5, i.e., at the maximal amounts of both Ag and Cu in the $\text{TiO}_2/\text{Ag}/\text{Cu}$ coating. The results of the MPN of surviving cells estimation confirm the findings obtained by the quick agar diffusion test (Table 3): higher sensitivity of *S. epidermidis* than *E. coli* to Ag NPs and Cu NPs dependent on the Ag and Cu concentration, and antimicrobial activity of the studied $\text{TiO}_2/\text{Ag}/\text{Cu}$ composite coatings.

Another demonstration of the specific antimicrobial activity of the studied $\text{TiO}_2/\text{Ag}/\text{Cu}$ composite coatings toward different bacterial species is evident in Figure 5, presenting the growth of different bacteria species in the presence of the same coating, Sample 5- $\text{TiO}_2/\text{Ag}_{23.1}\text{ at.}\%/\text{Cu}_{21.6}\text{ at.}\%$.

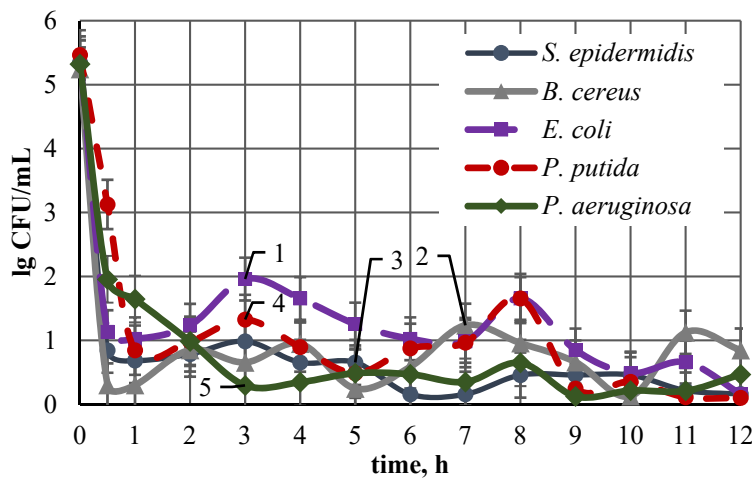


Figure 5. *E. coli* (curve 1), *B. cereus* (curve 2), *S. epidermidis* (curve 3), *P. putida* (curve 4), *P. aeruginosa* (curve 5) growth inhibition in presence of Sample 5- $\text{TiO}_2/\text{Ag}_{23.1}\text{ at.}\%/\text{Cu}_{21.6}\text{ at.}\%$.

The significant and specific antimicrobial activity of this coating toward large spectrum Gram-positive and Gram-negative microbial strains is clearly demonstrated by curves 1, 2, 3, 4, and 5. They show that the sharp decrease in the MPN of the surviving cells happens at different time intervals and it is down to different leaving cells number, both depending on the type of the microbial strain. The most sensitive to Ag/Cu as an antimicrobial agent is *S. epidermidis*, followed by *B. cereus*, *P. putida*, *P. aeruginosa* and *E. coli*.

3.5.3. *E. coli* Cells on Coated Glass Samples

Significant damage to and killing of *E. coli*, after growth on $\text{TiO}_2/\text{Ag}/\text{Cu}$ coated glass samples, were observed by SEM. Typical images are presented in Figure 6.

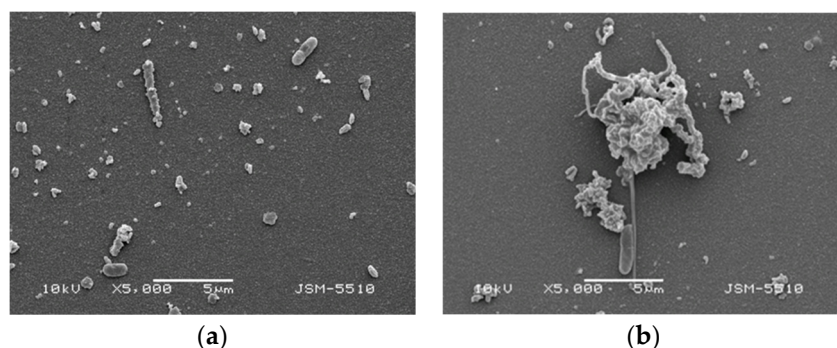


Figure 6. SEM images of significantly damaged *E. coli* cells (a) and *E. coli* cell aggregates (b) in contact with $\text{TiO}_2/\text{Ag}_{23.1}\text{ at.}\%/\text{Cu}_{21.6}\text{ at.}\%$ magnetron cosputtered composite coating.

Normally, the *E. coli* cells look like ovals with size of 0.8–1 μm . They seem to be damaged on the TiO₂/Ag/Cu coated samples: deformed, with elongated original shape, dehydrated surface and multiple indentations (Figure 6a,b). Large colonies of damaged *E. coli* cells are also observed in some places (Figure 6b). This could be due to a poured cell content, the last one not seen in these pictures, because it was eluted after the samples had been washed in distilled water. The SEM observation of the *E. coli* cells on the coated samples demonstrates their contact killing.

4. Discussion

The surfaces of all TiO₂/Ag/Cu coated samples (Samples 1–5) are characterized by similar morphology: Ag/Cu chainlike aggregates distributed chaotically in the coating (SEM, Figure 2b), and forming dark wells as visualized by the EDX maps (Figure 1b). All TiO₂/Ag/Cu coated samples are moderately hydrophilic (WCA of 63.0°–69.1°, Table 2). Both the observed surface morphology and the moderate hydrophilicity [58] of the studied coatings suppose good interactions with living cells, i.e., the observed suppression of the test microbial cells growth could not be due to a lack of the conditions for initial attachment (initial adhesion). The suppression of the microbial cells' growth by the studied TiO₂/Ag/Cu composite coatings and its extent is determined by the chemical composition of the coating, i.e., by the presence of the antimicrobial agent Ag/Cu and its concentration

The well expressed cell growth inhibition could be due to cellular interactions with presenting on or/and eluted from the coated surface, Ag and Cu nanoparticles, ions and reactive oxygen species formed as a result of the oxidative processes. It is known that Ag NPs and Ag⁺, Cu NPs and Cu²⁺ are active antibacterial agents, although that the mechanism of their antibacterial action is not fully understood [59]. Our experimental results demonstrate direct contact (SEM observation, Figure 6) and released silver/copper killing (diffusion assay, Table 2; MPN of living cells, Figures 3–5) of the bacterial cells by the studied TiO₂/Ag/Cu coatings. A similar mode of bactericidal action was proposed earlier for magnetron sputtered TiO₂ coatings, chemically incrusted with Ag NPs [12] and TiO₂/SiO₂/Ag magnetron cosputtered coatings [3,17].

There are a number of reports concerning the mechanism of action of Ag and Cu nanoparticles and ions. It was shown that silver ions (Ag⁺) interact with disulfide or sulphydryl groups of enzymes, which leads to the inhibition of metabolic processes [60,61]; silver binds bacterial DNA (deoxyribonucleic acid), inhibiting replication and transcription [62,63] and copper leads to the collapse of some lipopolysaccharide (LPS) patches and alters the permeability and functionality of the outer cell membrane [64]. It was demonstrated that the activity of the NPs is size [27,65] and shape-dependent [66]. The free NPs penetrate inside the bacteria after their attachment to the plasma membrane and interact with sulfur containing proteins and the phosphorus containing DNA, which leads to blockage of the cell division [67]. It is difficult to distinguish the bactericidal activity of the NPs from that of the metallic ions released by the nanoparticles [68]. It was reported that the combined effect of the adhesion and penetration of the NPs and ions is crucial for the biocidal effect, with the plasma membrane being the target of the rapid antibacterial action of the NPs in *E. coli* [69]. The NPs also interact with the cell envelope of *E. coli* [70]. Morphological analysis reveals that the hallmarks of cell damage and NP toxicity include an increase in cell surface roughness and a change of the shape and size of the cells [71], such as were observed in our study. The mechanism of the antimicrobial action of Cu NPs and ions is less studied and reports on the mechanism of antimicrobial action of such coexisting with Ag NPs and ions are scarce.

The bactericidal activity of the magnetron cosputtered TiO₂/Ag/Cu nanocomposite coatings could be due to a damage of the cell membrane and envelope (observed by SEM, Figure 6) usually resulting in a leakage of the cellular content, increased cell surface roughness, changed cell shape and size, and cell death [69–71]. The bonding of Ag NPs and Ag⁺, as well as of Cu NPs and Cu²⁺ from the studied coated samples to the microbial cells' proteins, could also contribute, inactivating the electron transport chain and thereby

inhibiting the respiration and growth of the cells, as was already reported [24]. The specific antimicrobial action of the studied coatings toward the used test bacterial strains could be explained with the specific features of their cells: rod or coil shape, presence or lack of flagella, cell envelope and membrane, density of the cell membrane, cell wall structure, etc. determining the engulf of the Ag/Cu NPs and ions [72,73].

The in-depth penetration of the mechanism of microbial cells' interactions with Ag NPs and Ag⁺, Cu NPs and Cu²⁺, as well as with simultaneously presenting Ag NPs/Cu NPs and Ag⁺/Cu²⁺, needs additional, more in-depth investigations.

5. Conclusions

This investigation combines Ag and Cu as dopants in RF cosputtered TiO₂/Ag/Cu functional coatings for medical devices and correlates their characteristics to the antimicrobial activity. The desired thickness, antibacterial activity and its durability can be obtained by the optimization of the operation parameters of the RF cosputtering and an accurately controlled composition of the TiO₂/Ag/Cu coatings, especially of the Ag and Cu content as dopants. The last one is a convenient tool for the adjustment of the balance between antimicrobial activity and cytotoxicity to the requirements of different medical devices.

The magnetron cosputtered TiO₂/SiO₂/Ag composite coatings demonstrate a wide spectrum of antimicrobial activity, suppressing significantly the growth of Gram-negative (*E. coli*, *P. aeruginosa*) and Gram-positive (*P. putida*, *B. cereus*, *S. epidermidis*) bacteria.

The cells' growth inhibition is specific and dependent on the Ag/Cu content for all used test bacterial strains. It is due to direct contact and eluted Ag/Cu-mediated killing, as experimentally demonstrated. The in-depth penetration in the mechanism of the microbial cells interaction with Ag and Cu nanoparticles and ions, as well as with simultaneously presented all of them needs in additional, more in-depth investigations.

It is expected that the studied magnetron cosputtered TiO₂/Ag/Cu coatings would ensure a broad spectrum of bactericidal activity during the indwelling of the coated medical devices and for at least 12 h after that, with the supposition that the benefits would continue over a longer time.

Author Contributions: T.V. conceptualized this investigation; D.G. and T.V. performed the data curation, funding acquisition, coatings characterization, writing and illustrations of the original draft; T.V. and D.G. performed the project administration; I.I. carried out the antimicrobial testing. All coauthors participated in the discussion of the experimental results. All authors have read and agreed to the published version of the manuscript.

Funding: Nation Scientific Fund, Bulgaria (Grants DCOST 01/4/2018; KP-06-COST/20/2019).

Institutional Review Board Statement: Not applicable.

Informed Consent Statement: Not applicable.

Data Availability Statement: Not applicable.

Acknowledgments: Nation Scientific Fund, Bulgaria is gratefully acknowledged for its financial support (Grants DCOST 01/4/2018; KP-06-COST/20/2019) of this investigation. It is a part of the activities of COST Action CA 16217 ENIUS. O. Angelov is acknowledged for the performance of the magnetron cosputtering just before retiring.

Conflicts of Interest: The authors declare no conflict of interest.

References

1. Ramstedt, M.; Ribeiro, I.A.C.; Bujdakova, H.; Mergulhão, F.J.M.; Jordao, L.; Thomsen, P.; Alm, M.; Burmølle, M.; Vladkova, T.; Can, F.; et al. Evaluating efficacy of antimicrobial and antifouling materials for urinary tract medical devices: Challenges and recommendations. *Macromol. Biosci.* **2019**, *19*, e1800384. [[CrossRef](#)] [[PubMed](#)]
2. Adlhart, C.; Verran, J.; Azevedo, N.F.; Olmez, H.; Keinänen-Toivola, M.M.; Gouveia, I.; Melo, L.F.; Crijns, F. Surface modifications for antimicrobial effects in the healthcare setting: A critical overview. *J. Hosp. Infect.* **2018**, *99*, 239–249. [[CrossRef](#)]
3. Murthy, S.P.; Raju, S.; Thiagarajan, V. *Biofilms Control: Biomedical and Industrial Environments*; Narosa Publishing House: New Delhi, India, 2019.

4. Khataee, A.; Mansoori, G.A. *Nanostructured Titanium Dioxide Materials*; World Scientific: Singapore, 2011. [CrossRef]
5. Kartini, I.; Khairani, I.Y.; Triyana, K.; Wahyuni, S. Nanostructured titanium dioxide for functional coatings. In *Titanium Dioxide: Material for a Sustainable Environment*; Intech Open: Rijeka, Croatia, 2018.
6. Watté, J.; Van Zele, M.; De Buysser, K.; Van Driessche, I. Recent advances in low-temperature deposition methods of transparent, photocatalytic TiO₂ coatings on polymers. *Coatings* **2018**, *8*, 131. [CrossRef]
7. Othman, S.H.; Salam, N.R.A.; Zainal, N.; Basha, R.K.; Talib, R.A. Antimicrobial activity of TiO₂ nanoparticle-coated film for potential food packaging applications. *Int. J. Photoenergy* **2014**, *2014*, 945930. [CrossRef]
8. Morrison, J. Copper’s Virus-Killing Powers were Known Even to the Ancients. Available online: <https://www.smithsonianmag.com/science-nature/copper-virus-kill-180974655/> (accessed on 14 April 2020).
9. Wilks, S.; Michels, H.; Keevil, C. The survival of escherichia coli o157 on a range of metal surfaces. *Int. J. Food Microbiol.* **2005**, *105*, 445–454. [CrossRef] [PubMed]
10. Mathews, S.; Hans, M.; Mücklich, F.; Solioz, M. Contact killing of bacteria on copper is suppressed if bacterial-metal contact is prevented and is induced on iron by copper ions. *Appl. Environ. Microbiol.* **2013**, *79*, 2605–2611. [CrossRef]
11. Mehtar, S.; Wiid, I.; Todorov, S. The antimicrobial activity of copper and copper alloys against nosocomial pathogens and mycobacterium tuberculosis isolated from healthcare facilities in the western cape: An in-vitro study. *J. Hosp. Infect.* **2008**, *68*, 45–51. [CrossRef]
12. Shimabukuro, M. Antibacterial property and biocompatibility of silver, copper, and zinc in titanium dioxide layers incorporated by one-step micro-arc oxidation: A review. *Antibiotics* **2020**, *9*, 716. [CrossRef]
13. Ning, C.; Wang, X.; Li, L.; Zhu, Y.; Li, M.; Yu, P.; Zhou, L.; Zhou, Z.; Chen, J.; Tan, G.; et al. concentration ranges of antibacterial cations for showing the highest antibacterial efficacy but the least cytotoxicity against mammalian cells: Implications for a new antibacterial mechanism. *Chem. Res. Toxicol.* **2015**, *28*, 1815–1822. [CrossRef]
14. Reidy, B.; Haase, A.; Luch, A.; Dawson, K.A.; Lynch, I. Mechanisms of silver nanoparticle release, transformation and toxicity: A critical review of current knowledge and recommendations for future studies and applications. *Materials* **2013**, *6*, 2295–2350. [CrossRef] [PubMed]
15. Marin, S.; Vlasceanu, G.M.; Tiplea, R.E.; Bucur, I.R.; Lemnaru, M.; Marin, M.M.; Grumezescu, A.M. Applications and toxicity of silver nanoparticles: A recent review. *Curr. Top. Med. Chem.* **2015**, *15*, 1596–1604. [CrossRef] [PubMed]
16. Petica, A.; Florea, A.; Gaidau, C.; Balan, D.; Anicai, L. Synthesis and characterization of silver-titania nanocomposites prepared by electrochemical method with enhanced photocatalytic characteristics, antifungal and antimicrobial activity. *J. Mater. Res. Technol.* **2019**, *8*, 41–53. [CrossRef]
17. Zawadzka, K.; Kisielewska, A.; Piwoński, I.; Kadzioła, K.; Felczak, A.; Różalska, S.; Wrońska, N.; Lisowska, K. Mechanisms of antibacterial activity and stability of silver nanoparticles grown on magnetron sputtered TiO₂ coatings. *Bull. Mater. Sci.* **2016**, *39*, 57–68. [CrossRef]
18. Brook, L.; Evans, P.; Foster, H.; Pemble, M.; Steele, A.; Sheel, D.; Yates, H. Highly bioactive silver and silver/titania composite films grown by chemical vapour deposition. *J. Photochem. Photobiol. A Chem.* **2007**, *187*, 53–63. [CrossRef]
19. Sheel, D.W.; Brook, L.A.; Ditta, I.B.; Evans, P.; Foster, H.A.; Steele, A.; Yates, H.M. Biocidal silver and silver/titania composite films grown by chemical vapour deposition. *Int. J. Photoenergy* **2008**, *2008*, 1–11. [CrossRef]
20. Page, K.; Palgrave, R.G.; Parkin, I.P.; Wilson, M.; Savin, S.L.P.; Chadwick, A.V. Titania and silver–titania composite films on glass—potent antimicrobial coatings. *J. Mater. Chem.* **2006**, *17*, 95–104. [CrossRef]
21. Nigussie, G.Y.; Tesfamariam, G.M.; Tegegne, B.M.; Weldemichel, Y.A.; Gebreab, T.W.; Gebrehiwot, D.G.; Gebremichel, G.E. Antibacterial activity of ag-doped TiO₂ and Ag-doped ZnO nanoparticles. *Int. J. Photoenergy* **2018**, *2018*, 5927485. [CrossRef]
22. Mangalaraj, D.; Nithya Devi, D. Ag/TiO₂ (Metal/Metal Oxide) Core Shell Nanoparticles for Biological Applications BT. In *Recent Trends in Materials Science and Applications*; Ebenezar, J., Ed.; Springer International Publishing: Cham, Switzerland, 2017; pp. 9–17.
23. Wahyuni, E.T.; Roto, R. Silver Nanoparticle Incorporated Titanium Oxide for Bacterial Inactivation and Dye Degradation. In *Titanium Dioxide: Material for a Sustainable Environment*; Intech Open: Rijeka, Croatia, 2018.
24. Vladkova, T.; Angelov, O.; Stoyanova, D.; Gospodinova, D.; Gomes, L.; Soares, A.; Mergulhao, F.; Ivanova, I. Magnetron co-sputtered TiO₂/SiO₂/Ag nanocomposite thin coatings inhibiting bacterial adhesion and biofilm formation. *Surf. Coat. Technol.* **2020**, *384*, 125322. [CrossRef]
25. Desai, V.; Kaler, S.G. Role of copper in human neurological disorders. *Am. J. Clin. Nutr.* **2008**, *88*, 855S–858S. [CrossRef]
26. Mungkalasiri, J.; Bedel, L.; Emieux, F.; Doré, J.; Renaud, F.; Maury, F. DLI-CVD of TiO₂–Cu antibacterial thin films: Growth and characterization. *Surf. Coat. Technol.* **2009**, *204*, 887–892. [CrossRef]
27. Mungkalasiri, J.; Bedel, L.; Emieux, F.; Doré, J.; Renaud, F.N.R.; Sarantopoulos, C.; Maury, F. CVD Elaboration of nanostructured TiO₂-Ag thin films with efficient antibacterial properties. *Chem. Vap. Depos.* **2010**, *16*, 35–41. [CrossRef]
28. Zielinska-Jurek, A.; Walicka, M.; Tadajewska, A.; Łacka, I.; Gazda, M.; Zaleska-Medynska, A. Preparation of Ag/Cu-doped titanium (IV) oxide nanoparticles in w/o microemulsion. *Physicochem. Probl. Miner. Process.* **2010**, *45*, 113–126.
29. Sangchay, W.; Lek, S.; Kooptarnond, K. The photocatalytic and antibacterial activity of Cu-doped TiO₂ thin films. *Walailak J. Sci. Technol.* **2013**, *10*, 19–27. [CrossRef]
30. Varghese, S.; ElFakhri, S.O.; Sheel, D.W.; Sheel, P.; Bolton, F.J.E.; Foster, H.A. Antimicrobial activity of novel nanostructured cu- SiO₂ coatings prepared by chemical vapour deposition against hospital related pathogens. *AMB Express* **2013**, *3*, 53. [CrossRef] [PubMed]

31. Wei, X.; Gao, W. Polymer-Cu/TiO₂ Antimicrobial Coatings BT. In *Proceedings of the 8th Pacific Rim International Congress on Advanced Materials and Processing*; Marquis, F., Ed.; Springer International Publishing: Cham, Switzerland, 2016; pp. 1663–1669.
32. Mungkalasiri, J.; Bedel, L.; Emieux, F.; Cara, A.V.-D.; Freney, J.; Maury, F.; Renaud, F.N. Antibacterial properties of TiO₂–Cu composite thin films grown by a one step DLICVD process. *Surf. Coat. Technol.* **2014**, *242*, 187–194. [CrossRef]
33. Krishnakumar, V.; Boobas, S.; Jayaprakash, J.; Rajaboopathi, M.; Han, B.; Louhi-Kultanen, M. Effect of Cu doping on TiO₂ nanoparticles and its photocatalytic activity under visible light. *J. Mater. Sci. Mater. Electron.* **2016**, *27*, 7438–7447. [CrossRef]
34. Zhang, L.; Guo, J.; Huang, X.; Zhang, Y.; Han, Y. The dual function of Cu-doped TiO₂ coatings on titanium for application in percutaneous implants. *J. Mater. Chem. B* **2016**, *4*, 3788–3800. [CrossRef] [PubMed]
35. Mathew, S.; Ganguly, P.; Rhatigan, S.; Kumaravel, V.; Byrne, C.; Hinder, S.J.; Bartlett, J.; Nolan, M.; Pillai, S.C. Cu-doped TiO₂: Visible light assisted photocatalytic antimicrobial activity. *Appl. Sci.* **2018**, *8*, 2067. [CrossRef]
36. Alavi, M.; Karimi, N. Antiplanktonic, antibiofilm, antiswarming motility and antiquorum sensing activities of green synthesized Ag–TiO₂, TiO₂–Ag, Ag–Cu and Cu–Ag nanocomposites against multi-drug-resistant bacteria. *Artif. Cells Nanomed. Biotechnol.* **2018**, *46*, S399–S413. [CrossRef] [PubMed]
37. Nißen, S.; Heeg, J.; Wienecke, M.; Behrend, D.; Warkentin, M.; Rokosz, K.; Gaiaschi, S.; Chapon, P. Surface characterization and copper release of a-C:H:Cu coatings for medical applications. *Coatings* **2019**, *9*, 119. [CrossRef]
38. Alotaibi, A.M.; Williamson, B.A.D.; Sathasivam, S.S.; Kafizas, A.; Alqahtani, M.; Sotelo-Vazquez, C.; Buckeridge, J.; Wu, J.; Nair, S.P.; Scanlon, D.O.; et al. Enhanced photocatalytic and antibacterial ability of Cu-Doped anatase TiO₂ thin films: Theory and experiment. *ACS Appl. Mater. Interfaces* **2020**, *12*, 15348–15361. [CrossRef] [PubMed]
39. Tahmasebizar, N.; Hamedani, M.T.; Ghazani, M.S.; Pazhuhanfar, Y. Photocatalytic activity and antibacterial behavior of TiO₂ coatings co-doped with copper and nitrogen via sol-gel method. *J. Sol. Gel Sci. Technol.* **2019**, *93*, 570–578. [CrossRef] [PubMed]
40. Behnajady, M.A.; Eskandarloo, H. Characterization and photocatalytic activity of Ag–Cu/TiO₂ nanoparticles prepared by sol-gel method. *J. Nanosci. Nanotechnol.* **2013**, *13*, 548–553. [CrossRef] [PubMed]
41. Yuan, W.; Ji, J.; Fu, J.; Shen, J. A facile method to construct hybrid multilayered films as a strong and multifunctional antibacterial coating. *J. Biomed. Mater. Res. Part B Appl. Biomater.* **2008**, *85*, 556–563. [CrossRef]
42. Akhavan, O. Lasting antibacterial activities of Ag–TiO₂/Ag/a-TiO₂ nanocomposite thin film photocatalysts under solar light irradiation. *J. Colloid Interface Sci.* **2009**, *336*, 117–124. [CrossRef]
43. Akhavan, O.; Ghaderi, E. Bactericidal effects of Ag nanoparticles immobilized on surface of SiO₂ thin film with high concentration. *Curr. Appl. Phys.* **2009**, *9*, 1381–1385. [CrossRef]
44. Mazur, M.; Wojcieszak, D.; Domaradzki, J.; Kaczmarek, D.; Song, S.; Placido, F. TiO₂/SiO₂ multilayer as an antireflective and protective coating deposited by microwave assisted magnetron sputtering. *Opt. Electron. Rev.* **2013**, *21*, 233–238. [CrossRef]
45. Khan, S.B.; Wu, H.; Pan, C.; Zhang, Z. A mini review: Antireflective coatings processing techniques, applications and future perspective. *Res. Rev. J. Mater. Sci.* **2017**, *5*, 1–19. [CrossRef]
46. Yamaguchi, T.; Tamura, H.; Taga, S.; Tsuchiya, S. Interfacial optical absorption in TiO₂–SiO₂ multilayer coatings prepared by rf magnetron sputtering. *Appl. Opt.* **1986**, *25*, 2703–2706. [CrossRef]
47. Vladkova, T.G.; Staneva, A.D.; Gospodinova, D.N. Surface engineered biomaterials and ureteral stents inhibiting biofilm formation and encrustation. *Surf. Coat. Technol.* **2020**, *404*, 126424. [CrossRef]
48. Gao, A.; Hang, R.; Chu, P.K. Recent advances in anti-infection surfaces fabricated on biomedical implants by plasma-based technology. *Surf. Coat. Technol.* **2017**, *312*, 2–6. [CrossRef]
49. Rijal, N. Most Probable Number (MPN) Test: Principle, Procedure and Results. Available online: <https://microbeonline.com/probable-number-mpn-test-principle-procedure-results/> (accessed on 11 June 2017).
50. Stoyanova, D.S.; Ivanova, I.A.; Angelov, O.I.; Vladkova, T.G. Antibacterial activity of thin films TiO₂ doped with Ag and Cu on gracilicutes and firmicutes bacteria. *Biodiscovery* **2017**, *20*, e15076. [CrossRef]
51. Wassmann, T.; Kreis, S.; Behr, M.; Buergers, R. The influence of surface texture and wettability on initial bacterial adhesion on titanium and zirconium oxide dental implants. *Int. J. Implant. Dent.* **2017**, *3*, 1–11. [CrossRef] [PubMed]
52. Poncin-Epaillard, F.; Vrlinic, T.; Debarnot, D.; Mozetic, M.; Coudreuse, A.; Legeay, G.; El Moualij, B.; Zorzi, W. Surface treatment of polymeric materials controlling the adhesion of biomolecules. *J. Funct. Biomater.* **2012**, *3*, 528–543. [CrossRef]
53. Speranza, G.; Gottardi, G.; Pederzolli, C.; Lunelli, L.; Canteri, R.; Pasquardini, L.; Carli, E.; Lui, A.; Maniglio, D.; Brugnara, M.; et al. Role of chemical interactions in bacterial adhesion to polymer surfaces. *Biomaterials* **2004**, *25*, 2029–2037. [CrossRef]
54. Vladkova, T.G. Surface engineered polymeric biomaterials with improved biocontact properties. *Int. J. Polym. Sci.* **2010**, *2010*, 296094. [CrossRef]
55. Vladkova, T.G. *Surface Engineering of Polymeric Biomaterials*; Smithers Rapra Technology: Shropshire, UK, 2013.
56. Ploux, L.; Ponche, A.; Anselme, K. Bacteria/material interfaces: Role of the material and cell wall properties. *J. Adhes. Sci. Technol.* **2010**, *24*, 2165–2201. [CrossRef]
57. Song, F.; Koo, H.; Ren, D. Effects of material properties on bacterial adhesion and biofilm formation. *J. Dent. Res.* **2015**, *94*, 1027–1034. [CrossRef]
58. Altankov, G. *Interaction of Cells with Biomaterial Surfaces*; Bulgarian Academy of Science: Sofia, Bulgaria, 2003.
59. Kędziora, A.; Speruda, M.; Krzyżewska, E.; Rybka, J.; Łukowiak, A.; Bugla-Płoskońska, G. Similarities and differences between silver ions and silver in nanoforms as antibacterial agents. *Int. J. Mol. Sci.* **2018**, *19*, 444. [CrossRef]

60. Feng, Q.L. A Mechanistic study of the antibacterial effect of silver ions on escherichia coli and staphylococcus Aureus. *J. Biomed. Mater. Res.* **2000**, *52*, 662–668. [[CrossRef](#)]
61. Butkus, M.A.; Edling, L.; Labare, M.P. The efficacy of silver as a bactericidal agent: Advantages, limitations and considerations for future use. *J. Water Supply Res. Technol.* **2003**, *52*, 407–416. [[CrossRef](#)]
62. Lansdown, A. Silver I: Its antibacterial properties and mechanism of action. *J. Wound Care* **2002**, *11*, 125–130. [[CrossRef](#)]
63. Castellano, J.J.; Shafii, S.M.; Ko, F.; Donate, G.; Wright, T.E.; Mannari, R.J.; Payne, W.G.; Smith, D.J.; Robson, M.C. Comparative evaluation of silver-containing antimicrobial dressings and drugs. *Int. Wound J.* **2007**, *4*, 114–122. [[CrossRef](#)] [[PubMed](#)]
64. Nan, L.; Liu, Y.; Lü, M.; Yang, K. Study on antibacterial mechanism of copper-bearing austenitic antibacterial stainless steel by atomic force microscopy. *J. Mater. Sci. Mater. Med.* **2008**, *19*, 3057–3062. [[CrossRef](#)]
65. Panáček, A.; Kvítek, L.; Prucek, R.; Kolář, M.; Večeřová, R.; Pizúrová, N.; Sharma, V.K.; Nevěcná, T.; Zbořil, R. Silver colloid nanoparticles: Synthesis, characterization, and their antibacterial activity. *J. Phys. Chem. B* **2006**, *110*, 16248–16253. [[CrossRef](#)]
66. Pal, S.; Tak, Y.K.; Song, J.M. Does the antibacterial activity of silver nanoparticles depend on the shape of the nanoparticle? A study of the gram-negative bacterium escherichia coli. *Appl. Environ. Microbiol.* **2007**, *73*, 1712–1720. [[CrossRef](#)]
67. Danilczuk, M.; Lund, A.; Sadlo, J.; Yamada, H.; Michalik, J. Conduction electron spin resonance of small silver particles. *Spectrochim. Acta Part A Mol. Biomol. Spectrosc.* **2006**, *63*, 189–191. [[CrossRef](#)]
68. Kim, J.S.; Kuk, E.; Yu, K.N.; Kim, J.-H.; Park, S.J.; Lee, H.J.; Kim, S.H.; Park, Y.K.; Park, Y.H.; Hwang, C.-Y.; et al. Antimicrobial effects of silver nanoparticles. *Nanomed. Nanotechnol. Biol. Med.* **2007**, *3*, 95–101. [[CrossRef](#)]
69. Bondarenko, O.M.; Sihtmäe, M.; Kuzmičiova, J.; Ragelienė, L.; Kahru, A.; Daugelavičius, R. Plasma membrane is the target of rapid antibacterial action of silver nanoparticles in escherichia coli and pseudomonas aeruginosa. *Int. J. Nanomed.* **2018**, *13*, 6779–6790. [[CrossRef](#)] [[PubMed](#)]
70. Sondi, I.; Salopek-Sondi, B. Silver nanoparticles as antimicrobial agent: A case study on *E. coli* as a model for gram-negative bacteria. *J. Colloid Interface Sci.* **2004**, *275*, 177–182. [[CrossRef](#)] [[PubMed](#)]
71. Prieto, E.; Kiat, A. The antimicrobial action of silver nanoparticles on *E. coli* as revealed by atomic force microscopy. *Philipp. Sci. Lett.* **2017**, *10*, 123–129.
72. Albu, M.G.; Vladkova, T.G.; Ivanova, I.A.; Shalaby, A.S.A.; Moskova-Doumanova, V.S.; Staneva, A.D.; Dimitriev, Y.B.; Kostadinova, A.S.; Topouzova-Hristova, T.I. Preparation and biological activity of new collagen composites, part I: Collagen/zinc titanate nanocomposites. *Appl. Biochem. Biotechnol.* **2016**, *180*, 177–193. [[CrossRef](#)] [[PubMed](#)]
73. Vladkova, T.G.; Ivanova, I.A.; Staneva, A.D.; Albu-Kaya, M.G.; Shalaby, A.S.A.; Moskova-Doumanova, V.; Kostadinova, A.S. Preparation and biological activity of new collagen composites, part III. collagen/(Ag/RGO) and collagen/(Ag/RGO/SiO₂) composites. *J. Arch. Mil. Med.* **2017**, in press. [[CrossRef](#)]